



CHORUS

This is the accepted manuscript made available via CHORUS. The article has been published as:

Coupling microwave photons to topological spin textures in math

Cu_2OSeO_3

S. Khan, O. Lee, T. Dion, C. W. Zollitsch, S. Seki, Y. Tokura, J. D. Breeze, and H. Kurebayashi

Phys. Rev. B **104**, L100402 — Published 3 September 2021

DOI: [10.1103/PhysRevB.104.L100402](https://doi.org/10.1103/PhysRevB.104.L100402)

1 **Coupling microwave photons to topological spin-textures in Cu_2OSeO_3**

2 S. Khan,^{1,*} O. Lee,¹ T. Dion,¹ C. W. Zollitsch,¹ S. Seki,² Y. Tokura,^{2,3,4} J. D. Breeze,⁵ and H. Kurebayashi^{1, †}

3 ¹*London Centre for Nanotechnology, University College London, London, WC1H 0AH, United Kingdom*

4 ²*Department of Applied Physics, University of Tokyo, Tokyo 113-8656, Japan*

5 ³*RIKEN Center for Emergent Matter Science (CEMS), Wako 351-0198, Japan*

6 ⁴*Tokyo College, University of Tokyo, Tokyo 113-8656, Japan*

7 ⁵*Department of Materials, Imperial College London,*
8 *Exhibition Road, London, SW7 2AZ, United Kingdom*

9 (Dated: August 13, 2021)

Abstract

Topologically protected nanoscale spin textures, known as magnetic skyrmions, possess particle-like properties and feature emergent magnetism effects. In bulk cubic heli-magnets, distinct skyrmion resonant modes are already identified using a technique like ferromagnetic resonance in spintronics. However, direct light-matter coupling between microwave photons and skyrmion resonance modes has not been demonstrated yet. Utilising two distinct cavity systems, we realise to observe a direct interaction between the cavity resonant mode and two resonant skyrmion modes, the counter-clockwise gyration and breathing modes, in bulk Cu_2OSeO_3 . For both resonant modes, we find the largest coupling strength at 57 K indicated by an enhancement of the cavity linewidth at the degeneracy point. We study the effective coupling strength as a function of temperature within the expected skyrmion phase. We attribute the maximum in effective coupling strength to the presence of a large number of skyrmions, and correspondingly to a completely stable skyrmion lattice. Our experimental findings indicate that the coupling between photons and resonant modes of magnetic skyrmions depends on the relative density of these topological particles instead of the pure spin number in the system.

INTRODUCTION

In condensed matter physics, the study of light-matter interactions holds an important stature as it provides physical insight into properties of coupled systems while facilitating the design of new-concept devices¹⁻³. The light-matter coupling in this context between microwave photons residing in a cavity and particle ensembles has been studied in a wide range of material systems⁴. These systems include two-dimensional electron gases^{5,6}, paramagnetic spins^{7,8} and exchange interaction dominated ordered spin systems⁹⁻¹². Quantum information processing as quantum memories^{13,14} and quantum transducers¹⁵ are particularly interesting applications which could be made possible due to the hybrid spin-ensemble-photon systems. Formation of a quasi-particle, known as the cavity-magnon-polariton (CMP), results from the strong coherent coupling phenomenon between cavity photons and magnons (i.e. a quanta of spin-waves) creating a hybridised state between the two¹⁶. One main advantage for using ferromagnetic materials as a base for spin-photon hybrid systems is the large spin number (N), as this yields very sizeable collective coupling strength (g_c) between the two systems due to the scaling condition given as $g_c = g_0\sqrt{N}$, where g_0 is the single spin - single photon coupling strength^{17,18}.

In our earlier work¹⁹, we demonstrated the existence of a stable polariton state by achieving strong coupling between cavity photons and magnons in the field-polarised phase of Cu_2OSeO_3 . We also observed dispersive coupling between cavity photons and heli-magnons in the non-collinear phases (helical and conical phases). Cu_2OSeO_3 is a material system well known to host another exotic topologically protected spin texture state known as magnetic skyrmions²⁰, which stabilise as a skyrmion lattice in a narrow temperature region below the Curie temperature, T_c . It has been shown that the skyrmion lattice can be excited by magnetic resonance techniques^{21,22}, where the resonance comprises of a collective skyrmion core precession in the counter-clockwise (CCW) and clockwise directions (gyration modes), and the breathing mode where skyrmion cores periodically shrink and enlarge. An open question was left unanswered in our previous work¹⁹, what happens when the cavity photons try to couple with the excitations of a skyrmion lattice? The difficulty in answering this question was mainly due to the high cavity resonance frequency (≈ 9 GHz), where a direct interaction with the skyrmion resonance modes ($\approx 1 - 2$ GHz) could not be observed.

In this study, we designed two separate cavity systems each optimised to explore the interaction between the cavity and the skyrmion excitation modes. Both cavities are designed to have their primary resonant modes within the expected frequency window of either the CCW or breathing skyrmion modes. We observe the onset of an avoided crossing of the cavity mode, indicating the interaction of the cavity with the skyrmion system by shifting the cavity mode significantly. An enhancement in the cavity linewidth is observed at the degeneracy point, where cavity and skyrmion modes cross. By probing the cavity linewidth as a function of external magnetic field we are able to deduce the effective coupling strength as well as the effective loss rate of the skyrmion excitation. A detailed temperature dependence of the effective coupling strength is extracted for both the CCW and breathing skyrmion modes, indicating the presence of a large number of skyrmions in the vicinity of 57 K. At this temperature the effective coupling strength is largest and we find the cavity-skyrmion hybrid system in the high cooperativity regime.

EXPERIMENTAL PROCEDURE

Figure 1(a) shows the schematic to highlight the interaction picture between photons (with a loss rate κ_c) and skyrmion resonant modes (with an effective loss rate γ_{sky}), with g_c representing the effective coupling rate between the two excited systems. The dielectric strontium titanate (STO) and helical (helically wrapped copper wire) resonator are used to study the coupling of microwave photons with the counterclockwise (CCW) and breathing skyrmion modes, respectively, in Cu_2OSeO_3 . The remaining of Fig. 1 shows the experimental setup for the (b) STO and (c) helical resonator (see supplementary material for full description²³). The resonance frequency of the primary mode ($\text{TE}_{01\delta}$) of

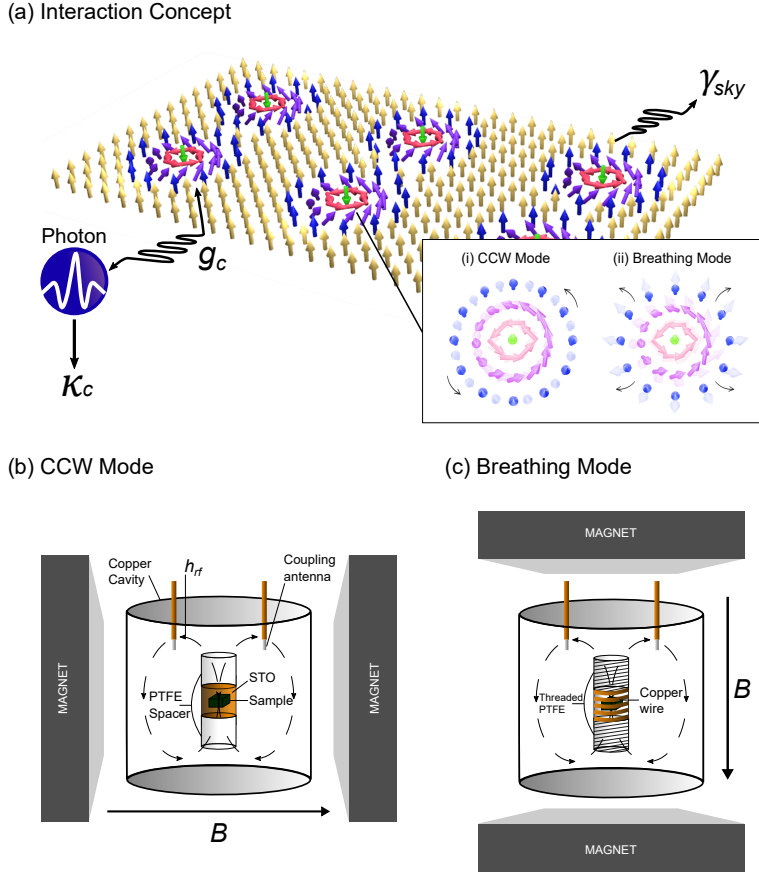


FIG. 1. (a) Illustration of the interaction between photons and excitation modes of skyrmion lattice showing the resonant motions of (i) CCW mode where the core of skyrmion rotates, and (ii) breathing mode which involves a periodic oscillation of the skyrmion core diameter. Schematic view of the experimental setup used with the (b) STO cavity where $\mathbf{h}_{rf} \perp \mu_0 \mathbf{H}$ for CCW mode, and (c) helical resonator where $\mathbf{h}_{rf} \parallel \mu_0 \mathbf{H}$ for breathing mode. The cavity and resonator are held in the helium-4 cryostat, and the cryostat sat in between the poles of the electromagnet. A Cu_2OSeO_3 sample is placed inside the STO cavity and helical resonator with the support of PTFE spacers and threaded PTFE tube, respectively. The coupling to cavity/resonator is achieved by connecting two microwave lines from the vector network analyser (VNA) to the coupling loops in the copper cavity.

63 the STO cavity, $\omega/2\pi \approx 1.1$ GHz at 57 K is in the expected range of the CCW excitation, as expected from broadband
 64 ferromagnetic resonance (FMR) measurements (see supplementary materials)²¹. One can only excite the breathing
 65 mode when the microwave magnetic field in the cavity (\mathbf{h}_{rf}) is parallel to the external magnetic field ($\mu_0 \mathbf{H}$)²², as shown
 66 in Fig. 1(c). This is achieved by exciting the primary mode of the helical resonator with an excitation frequency,
 67 $\omega/2\pi \approx 1.4$ GHz. In the parallel excitation configuration, the excitation of all the other magnetic resonant modes in
 68 Cu_2OSeO_3 should be suppressed, and the resonator mode is expected only to couple to the breathing mode.

69 RESULTS & DISCUSSION

70 Onset of an avoided crossing effect in skyrmion phase

71 Figure 2(a) shows the microwave transmission, $|S_{21}|^2$, as a function of ($\mu_0 \mathbf{H}$) and probe frequency for the CCW
 72 skyrmion mode at 57 K. The observed spectra exhibit a strong dependence of the cavity mode on $\mu_0 \mathbf{H}$ and a clear shift
 73 in the resonance frequency is seen within the field region where a skyrmion lattice is expected. This shift represents
 74 an onset of an avoided crossing, due to the coupling of the cavity mode to the skyrmion excitations. A complete
 75 avoided crossing, where the cavity resonant mode splits into two peaks in frequency, indicates strong coupling²⁴. The
 76 splitting corresponds to a hybridisation of the two systems, where the separation relates to the coupling strength.
 77 The linewidth of the two peaks is defined by the average of the linewidth of the two subsystems. If the linewidth or

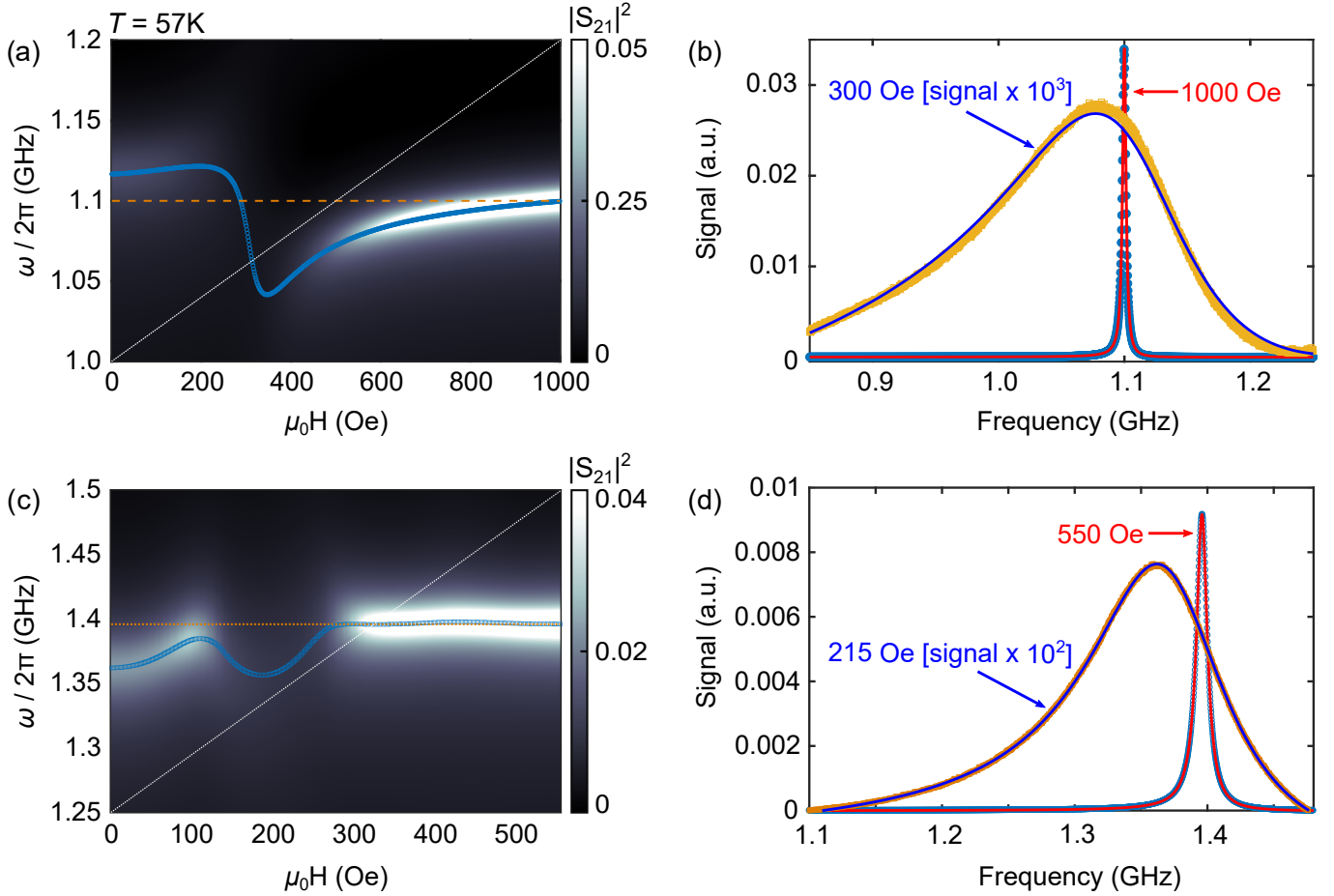


FIG. 2. The experimentally measured microwave transmission spectra, $|S_{21}|^2$, at 57 K for (a) CCW mode and (c) breathing mode, **where no background subtraction is performed for the data shown here**. The dashed orange line represents the cavity mode, and the resonance peak position plotted as circles (blue). (b) and (d) show line cuts in the frequency domain at high magnetic field away from skyrmion resonance and at field region in the interaction point for CCW and breathing mode, respectively. The data are fitted with a Lorentzian function.

78 loss rates of either one or both subsystems is larger than the coupling strength, the two peaks merge. This is the
 79 case of the cavity-skyrmion hybrid system we here investigate. In the following, we determine the effective coupling
 80 strength and effective skyrmion loss rate to classify the regime of coupling.

81 In Fig. 2(a), $|S_{21}|^2$ drops significantly in the field region between 150 Oe to 400 Oe (*i.e. in the expected field
 82 region of the CCW mode at 57 K²², and also shown in supplementary materials through the co-planar waveguide
 83 FMR measurements*). To study the evolution of cavity resonance frequency and linewidth in greater detail, we fit a
 84 Lorentzian line shape for each magnetic field in the frequency domain²⁵. Figure 2(b) shows the fitted spectrum at
 85 1000 Oe and in the gap area (300 Oe). The extracted resonance peak position is plotted (blue circles) in Fig. 2(a).
 86 A large increase in linewidth of the cavity mode is visible when Cu_2OSeO_3 is in the skyrmion phase. Note, that we
 87 are observing a single broad lineshape instead of two separated peaks, indicating that the hybrid system exhibits loss
 88 rates larger than the coupling strength²⁶.

89 Figure 2(c) shows the microwave transmission where the breathing skyrmion mode and the photon mode of the
 90 helical resonator interact at 57 K. As in the case of the CCW skyrmion excitation mode, $|S_{21}|^2$ exhibits a decrease in
 91 intensity, in a magnetic field space covering the skyrmion phase. The microwave transmission as a function of probe
 92 frequency for magnetic fields on and far away from the skyrmion resonance are shown in Fig. 2(d). By following the
 93 same procedure of fitting a Lorentzian function in the frequency domain for each magnetic field, similarly to the CCW
 94 case, a clear resonance frequency shift and linewidth broadening is observed.

95 It is evident from Fig. 2(a) and (c), that the photon modes in the STO cavity and the helical resonator couple to
 96 the excitation modes of the skyrmion lattice, *i.e.* CCW gyration and breathing mode, respectively. This is further
 97 supported by measurements at temperatures outside of the skyrmion phase ($T < T_{\text{sky}} < T_c$ and $T > T_c$). Here the
 98 cavity modes show no signature of coupling in resonance frequency or linewidth (respective colour plots shown in

99 supplementary material²³).

100 Temperature dependence of coupling strength

101 To identify the epitome of coupling between photons and skyrmion resonance, we analysed the linewidth dependence
 102 of the cavity as a function of $\mu_0\mathbf{H}$ for both CCW and breathing modes. According to the two coupled harmonic
 103 oscillators model^{12,27–30}, the cavity linewidth (half-width at half-maximum), $\kappa_{(S/H)}$ (S: STO cavity and H: helical
 104 resonator), is given by the following Lorentzian profile, as

$$\kappa_{(S/H)} = \kappa_c + \frac{g_c^2 \gamma_{\text{sky}}}{(\Delta^2 + \gamma_{\text{sky}}^2)} \quad (1)$$

105 where κ_c represents the loss rate of the cavity photons, γ_{sky} is the effective loss rate for skyrmion resonance, g_c
 106 is the effective coupling rate between the photons and skyrmion excitations, and Δ is the field dependent detuning,
 107 given as $\Delta = \frac{g\mu_0\mu_B}{\hbar}[\mathbf{H} - \mathbf{H}_{\text{res}}]$, with g being the g-factor of the sample, taken as $g = 2.1$ for Cu_2OSeO_3 ²².

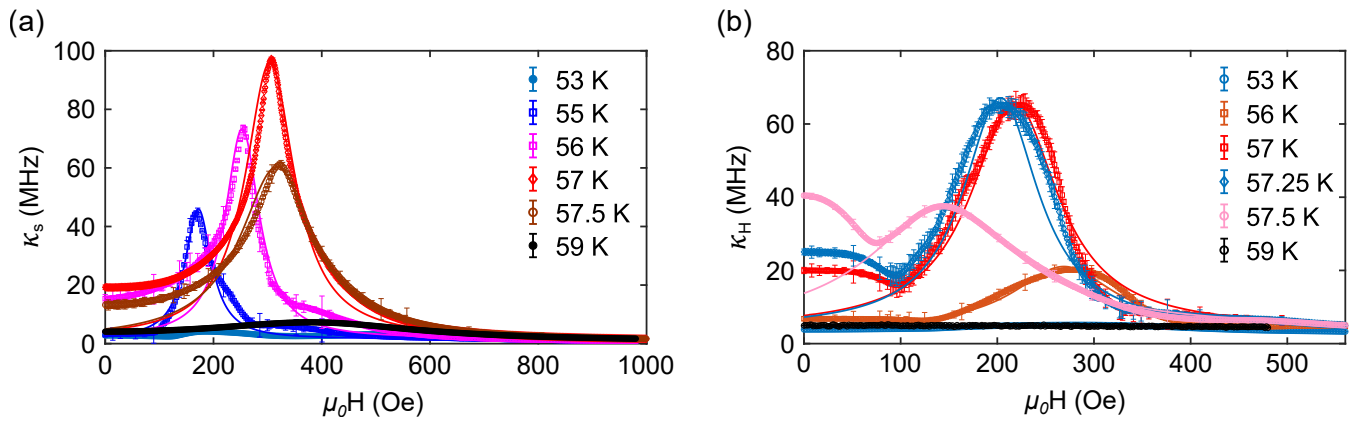


FIG. 3. Shows the experimentally extracted linewidth (HWHM) of (a) the STO cavity interacting with CCW mode and (b) helical resonator coupling to the breathing mode as a function of external magnetic field for different temperatures. The data in both is fitted with Equation 1 in the main text.

108 Figures 3(a) and (b) show the evolution of the extracted linewidth as a function of $\mu_0\mathbf{H}$ at different temperatures for
 109 the CCW and breathing skyrmion modes, respectively. It is clearly noticeable that in both cases $\kappa_{(S/H)}$ shows a peak
 110 like behaviour. At high magnetic fields, the photon mode in the STO cavity and the helical resonator is decoupled
 111 from the magnetic system and the measured linewidth mainly remains constant. A large deviation in the linewidth
 112 is observed as the magnetic field approaches the expected field region for the skyrmion lattice in the phase diagram
 113 at given temperatures. For temperatures outside of the skyrmion phase, i.e. 53 K ($T < T_{\text{sky}}$) and 59 K ($T > T_c$), we
 114 observe no significant change in linewidth as can be seen in Fig. 3(a) and (b). This provides strong evidence that the
 115 photon mode couples to the skyrmion resonance modes.

116 In the skyrmion phase, for both CCW and breathing modes, a fit to the data in Figs 3(a) and (b) is performed using
 117 Eq 1 with κ_c , γ_{sky} and g_c as free parameters. The largest effective coupling strength is observed at 57 K for CCW
 118 and breathing skyrmion modes. The extracted fitting parameters at 57 K are $g_c^{\text{ccw}}/2\pi = 118$ MHz, $\gamma_{\text{sky}}/2\pi = 250$
 119 MHz and $\kappa_c^{\text{sto}}/2\pi = 1.5$ MHz for the CCW mode, and $g_c^{\text{br}}/2\pi = 108$ MHz, $\gamma_{\text{sky}}/2\pi = 309$ MHz and $\kappa_c^{\text{heli}}/2\pi = 4$ MHz
 120 for the breathing mode.

121 The type of coupling observed between photons and skyrmion resonance modes falls in a regime where $\kappa_c < g_c < \gamma_{\text{sky}}$
 122 for both CCW and breathing modes. The skyrmion resonance is heavily damped such that the rate of excitation loss
 123 happens at a faster rate so that the energy cannot be transferred back and forth between the photon and skyrmion
 124 systems. This is illustrated in the schematic shown as an inset in Fig. 4, where the driven photon system ($|10\rangle$) coupled
 125 to the skyrmion resonant mode ($|01\rangle$) opens up an additional path back to the ground state ($|00\rangle$). This results in an
 126 enhancement of the linewidth ($\kappa_{(S/H)}$) of the microwave cavity due to its coupling to the skyrmion resonant modes.

127 Figure 4 shows the temperature dependence of g_c extracted from the linewidth analysis for both CCW and breathing
 128 skyrmion modes. As mentioned earlier, in Cu_2OSeO_3 , the skyrmion phase is expected to exist in a narrow temperature
 129 range below T_c . We see that for both CCW and breathing modes, the highest effective coupling strength is observed

130 for a 1 K range centered around 57 K. The effective coupling strength gradually falls down when the system is further
 131 cooled, and no coupling is observed at 53 K where the linewidth of the STO cavity and the helical resonator becomes
 132 unaffected. The experimentally observed trend in the temperature dependence of the effective coupling strength is
 133 asymmetric. Above 57.5 K, there is a sharp decrease in g_c , reflective of a transition from an ordered magnetic state
 134 to the paramagnetic state.

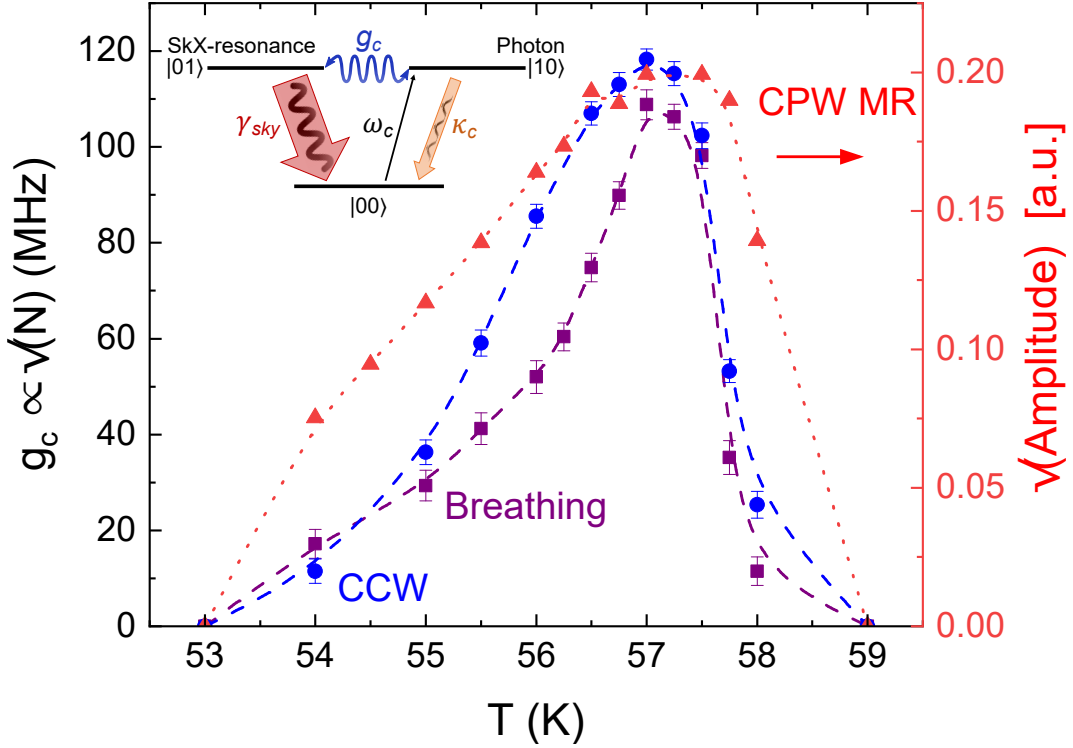


FIG. 4. (Left y-axis) Shows the effective coupling strength g_c as a function of temperature for CCW mode (blue circles) and breathing mode (purple squares). (Right y-axis) Shows the temperature dependence of the square-root amplitude of resonance peaks extracted from the CPW magnetic resonance experiment. The inset shows a schematic illustrating an interaction between photons and skyrmion excitation. $|00\rangle$ corresponds to the ground state where no photons or skyrmion excitation exists in the cavity, when driven by microwave power, the cavity enters the excited state $|10\rangle$. Coupling of $|10\rangle$ with the excited skyrmion state $|01\rangle$ with coupling strength g_c increases the cavity loss rate by having an additional damped channel through skyrmions. The dashed lines are for eye guidance.

135 It is well established that the coupling between photons and an ensemble of spins scales with the square-root of the
 136 thermally polarised number of spins (N) involved in the interaction, $g_c \propto \sqrt{N}$ ³¹. We anticipate that for interpreting
 137 the results shown in Fig. 4, one has to think of the coupling between photons and skyrmion resonance being dependent
 138 on the effective number of skyrmions taking part in the interaction. This suggests that around 57 K, a stable hexagonal
 139 skyrmion lattice is present, resulting in a greater number of skyrmions. As we move away from this centered region of
 140 the skyrmion phase, the number of skyrmions decrease resulting in a mixed state of magnetic domains and skyrmions.
 141 Hence, we see a decrease in the coupling strength between photons and skyrmion resonance. This is further supported
 142 by the temperature dependence of the intensity of small-angle neutron scattering (SANS) and the relaxation rate of
 143 muon-spin relaxation measurements in Cu_2OSeO_3 ^{32–34}, where the intensity and relaxation rate, respectively, have a
 144 maximum around 57 K and a drop was observed at different temperatures in the skyrmion phase.

145 In order to further elaborate on the above interpretation, we carried out co-planar waveguide (CPW) magnetic
 146 resonance measurements in the skyrmion phase on the same sample used for the cavity experiments (see supplementary
 147 material²³). The intensity ($I \propto \text{amplitude}$) of the magnetic resonance peak is proportional to the magnetisation in the
 148 system³⁵. In turn, probing the intensity, here mainly governed by the skyrmion population and the effective amplitude
 149 of local magnetic moment under thermal fluctuation, in the skyrmion phase of Cu_2OSeO_3 should be an indicator of
 150 the effective number of skyrmions contributing to the magnetic resonance peak amplitude at any given temperature.
 151 Therefore, the temperature dependence of the square-root amplitude of the magnetic resonance peaks can reflect the
 152 trend seen in the effective coupling strength, i.e. $g_c \propto \sqrt{N}$. Figure 4 (right y-axis) shows the square-root of the
 153 amplitude of CPW magnetic resonance peaks as a function of T . The maximum value of the amplitude is observed

154 in the vicinity of 57 K, and is qualitatively similar to the trend observed in g_c for a narrow temperature region where
155 a stable hexagonal skyrmion lattice in Cu_2OSeO_3 is expected.

156 In cavity QED, the cooperativity is a dimensionless figure of merit for the coupling strength given as $C =$
157 $g_c^2/\kappa_c\gamma_{\text{sky}}$ ¹², with $C > 1$ being a condition to achieve coherent coupling. In this work, the largest effective cou-
158 pling strength value results in $C = 37$ for the coupling of STO cavity photons to the CCW skyrmion mode and $C = 10$
159 for the coupling between the helical resonator photons and the breathing skyrmion mode. In both cases, an unstable
160 polariton state is created between photons and skyrmion resonance, coined as a regime of high cooperativity. At
161 resonance nearly all photons inside the cavity are coherently transferred into skyrmion excitations, but transferring
162 the excitations back will require a skyrmion resonance system with a smaller loss rate (i.e. $\gamma_{\text{sky}} < g_c$). An earlier
163 theoretical study on the coupling of photons to a breathing skyrmion mode in a thin magnetic disc does conclude
164 that reaching the strong coupling condition in such a system is challenging due to the large loss rate of the skyrmion
165 modes³⁶.

166 In conclusion, we have probed the type of coupling between photons in either a STO cavity or a helical resonator
167 to the CCW and breathing skyrmion modes in Cu_2OSeO_3 , respectively. At resonance, an onset of avoided crossing
168 effect is observed, indicating an interaction between the photon mode and skyrmion modes. An enhancement in
169 linewidth at the degeneracy point reveals that the system is in a regime of high cooperativity with $\kappa_c < g_c < \gamma_{\text{sky}}$
170 for both CCW and breathing modes. The effective coupling strength exhibits a distinct dependence on temperature
171 within the skyrmion phase, and comparing it with the amplitude of CPW magnetic resonance measurements confirms
172 the presence of a skyrmion lattice with a maximum effective number of skyrmions within the vicinity of 57 K. For
173 photon-magnon interactions, the coupling strength scales with the square-root of the number of thermally polarised
174 spins/particles. This study reveals that the interaction between photons and resonant modes of topological spin
175 structures strongly depends on the density of these topological particles instead of the pure spin number in the
176 system. It seems challenging to theoretically predict the number of skyrmions in a bulk system like Cu_2OSeO_3 , with
177 difficulty in an accurate determination of the temperature dependence of internal demagnetisation fields, anisotropy
178 fields, exchange and Dzyaloshinskii-Moriya interactions, and taking into account the quantum effects from spins. A
179 reliable theory support can allow this coupling technique to be used in future as an experimental determination of
180 the number of skyrmions in a given system.

181 *Note:* In the preparation of this manuscript, authors came to know of the recent pre-print study of dispersive
182 coupling, away from the resonance frequency of skyrmion excitations, between skyrmion modes and cavity photon
183 mode, with a high cooperativity observed at 56.5 K³⁷.

184 ACKNOWLEDGEMENTS

185 The research was supported by JSPS Grants-In-Aid for Scientific Research (Grant Nos. 18H03685, 20H00349,
186 21H04440), JST PRESTO (Grant No. JPMJPR18L5), Asahi Glass Foundation and JST CREST (Grant No. JP-
187 MJCR1874). We would like to thank Mr. Langdon (UCL EEE workshop) for making parts to place the cavity system
188 inside of the cryostat. We are grateful to Prof. Mochizuki for the helpful discussions.

189 * safe.khan.11@ucl.ac.uk

190 † h.kurebayashi@ucl.ac.uk

191 ¹ Y. Li, W. Zhang, V. Tyberkevych, W.-K. Kwok, A. Hoffmann, and V. Novosad, *Journal of Applied Physics* **128**, 130902
192 (2020).

193 ² A. Clerk, K. Lehnert, P. Bertet, J. Petta, and Y. Nakamura, *Nature Physics* **16**, 257 (2020).

194 ³ D. D. Awschalom, C. Du, R. He, F. Heremans, A. Hoffmann, J. Hou, H. Kurebayashi, Y. Li, L. Liu, V. Novosad, *et al.*,
195 arXiv preprint arXiv:2102.03222 (2021).

196 ⁴ B. Bhoi and S.-K. Kim, *Solid State Physics* **70**, 1 (2019).

197 ⁵ V. Muravev, I. Andreev, I. Kukushkin, S. Schmult, and W. Dietsche, *Physical Review B* **83**, 075309 (2011).

198 ⁶ G. Scalari, C. Maissen, D. Turčinková, D. Hagenmüller, S. De Liberato, C. Ciuti, C. Reichl, D. Schuh, W. Wegscheider,
199 M. Beck, *et al.*, *Science* **335**, 1323 (2012).

200 ⁷ I. Chiorescu, N. Groll, S. Bertaina, T. Mori, and S. Miyashita, *Physical Review B* **82**, 024413 (2010).

201 ⁸ J. D. Breeze, E. Salvadori, J. Sathian, N. M. Alford, and C. W. Kay, *npj Quantum Information* **3**, 1 (2017).

202 ⁹ Y. Tabuchi, S. Ishino, T. Ishikawa, R. Yamazaki, K. Usami, and Y. Nakamura, *Physical review letters* **113**, 083603 (2014).

203 ¹⁰ X. Zhang, C.-L. Zou, L. Jiang, and H. X. Tang, *Physical review letters* **113**, 156401 (2014).

204 ¹¹ M. Goryachev, W. G. Farr, D. L. Creedon, Y. Fan, M. Kostylev, and M. E. Tobar, *Physical Review Applied* **2**, 054002
205 (2014).

206 ¹² H. Huebl, C. W. Zollitsch, J. Lotze, F. Hocke, M. Greifenstein, A. Marx, R. Gross, and S. T. Goennenwein, *Physical Review Letters* **111**, 127003 (2013).

207 ¹³ R. Schoelkopf and S. Girvin, *Nature* **451**, 664 (2008).

208 ¹⁴ G. Kurizki, P. Bertet, Y. Kubo, K. Mølmer, D. Petrosyan, P. Rabl, and J. Schmiedmayer, *Proceedings of the National Academy of Sciences* **112**, 3866 (2015).

209 ¹⁵ S. Blum, C. O'Brien, N. Lauk, P. Bushev, M. Fleischhauer, and G. Morigi, *Physical Review A* **91**, 033834 (2015).

210 ¹⁶ M. Harder and C.-M. Hu, *Solid State Physics* **69**, 47 (2018).

211 ¹⁷ G. Agarwal, *Physical review letters* **53**, 1732 (1984).

212 ¹⁸ A. Imamoglu, *Physical review letters* **102**, 083602 (2009).

213 ¹⁹ L. Abdurakhimov, S. Khan, N. Panjwani, J. Breeze, M. Mochizuki, S. Seki, Y. Tokura, J. Morton, and H. Kurebayashi, *Physical Review B* **99**, 140401 (2019).

214 ²⁰ Y. Okamura, F. Kagawa, M. Mochizuki, M. Kubota, S. Seki, S. Ishiwata, M. Kawasaki, Y. Onose, and Y. Tokura, *Nature communications* **4**, 1 (2013).

215 ²¹ Y. Onose, Y. Okamura, S. Seki, S. Ishiwata, and Y. Tokura, *Physical review letters* **109**, 037603 (2012).

216 ²² T. Schwarze, J. Waizner, M. Garst, A. Bauer, I. Stasinopoulos, H. Berger, C. Pfeleiderer, and D. Grundler, *Nature materials* **14**, 478 (2015).

217 ²³ See Supplemental Materials at [URL will be inserted by publisher] for detailed experimental method, VNA calibration, cavity measurements outside of skyrmion phase and CPW magnetic resonance experiment.

218 ²⁴ D. Lachance-Quirion, Y. Tabuchi, A. Gloppe, K. Usami, and Y. Nakamura, *Applied Physics Express* **12**, 070101 (2019).

219 ²⁵ S. S. Kalarickal, P. Krivosik, M. Wu, C. E. Patton, M. L. Schneider, P. Kabos, T. J. Silva, and J. P. Nibarger, *Journal of Applied Physics* **99**, 093909 (2006).

220 ²⁶ L. Bai, K. Blanchette, M. Harder, Y. Chen, X. Fan, J. Xiao, and C.-M. Hu, *IEEE Transactions on Magnetics* **52**, 1 (2016).

221 ²⁷ S. Haroche and J.-M. Raimond, *Exploring the quantum: atoms, cavities, and photons* (Oxford university press, 2006).

222 ²⁸ P. F. Herskind, A. Dantan, J. P. Marler, M. Albert, and M. Drewsen, *Nature Physics* **5**, 494 (2009).

223 ²⁹ E. Abe, H. Wu, A. Ardavan, and J. J. Morton, *Applied Physics Letters* **98**, 251108 (2011).

224 ³⁰ G. Dold, C. W. Zollitsch, J. Osullivan, S. Welinski, A. Ferrier, P. Goldner, S. de Graaf, T. Lindström, and J. J. Morton, *Physical Review Applied* **11**, 054082 (2019).

225 ³¹ C. W. Zollitsch, K. Mueller, D. P. Franke, S. T. Goennenwein, M. S. Brandt, R. Gross, and H. Huebl, *Applied Physics Letters* **107**, 142105 (2015).

226 ³² T. Adams, A. Chacon, M. Wagner, A. Bauer, G. Brandl, B. Pedersen, H. Berger, P. Lemmens, and C. Pfeleiderer, *Physical Review Letters* **108**, 237204 (2012).

227 ³³ S. Seki, J.-H. Kim, D. Inosov, R. Georgii, B. Keimer, S. Ishiwata, and Y. Tokura, *Physical Review B* **85**, 220406 (2012).

228 ³⁴ T. Hicken, M. Wilson, K. Franke, B. Huddart, Z. Hawkhead, M. Gomilšek, S. Clark, F. Pratt, A. Štefančič, A. Hall, *et al.*, *Physical Review B* **103**, 024428 (2021).

229 ³⁵ M. Farle, *Reports on progress in physics* **61**, 755 (1998).

230 ³⁶ M. J. Martínez-Pérez and D. Zueco, *New Journal of Physics* **21**, 115002 (2019).

231 ³⁷ L. Liensberger, F. X. Haslbeck, A. Bauer, H. Berger, R. Gross, H. Huebl, C. Pfeleiderer, and M. Weiler, *arXiv preprint arXiv:2102.11713* (2021).

232

233

234

235

236

237

238

239

240

241

242

243